# Role of Adaptive Discretization in a Freeway Simulation Model

PHILIP S. BABCOCK IV, DAVID M. AUSLANDER, MASAYOSHI TOMIZUKA, and ADOLF D. MAY

ABSTRACT

Preliminary studies with the FREFLO freeway simulation model showed it to have difficulty depicting congested flow situations. This problem is traced to the model's transformation from the continuous to the discrete domain. Methods of determining the proper discretization intervals are shown along with simulation examples of a simple freeway. The properly discrete model requires an excessive amount of computer time for a real freeway simulation. Hence, two adaptive schemes that reduce the computing time to a manageable level are presented. The resulting model, FRECON, is then calibrated and validated using five peak-period data sets from the Santa Monica Freeway in Los Angeles.

Simulation models can serve many purposes in the understanding and design of traffic systems. They allow experiments to be conducted conveniently and safely. Insights into the functional relationships of various system elements can be gained through modeling, and future conditions may be predicted based on current system behavior.

This work in simulation models was motivated by the need to compare freeway performance under different control schemes and to aid in the design of new control strategies (1). For these uses a freeway simulation model must give an accurate representation of freeway speeds, densities, and flow rates as a function of demands and geometry. The wide range of time scales used in the control strategies studied (ranging from less than 1 minute to 15 minutes) required a dynamic model. Because freeway on-ramp control usually uses data derived from bulk properties of the resulting freeway flow, macroscopic freeway models would provide sufficient resolution for this work.

The FREFLO model was selected as the basis for the simulation study. The model, developed by Payne (2,3), is macroscopic and dynamic. Preliminary work with the model, along with a discussion presented elsewhere (4), revealed a serious deficiency in the model's ability to simulate congested flows in a realistic fashion. This problem was traced to the transformation of the model's formulation from the continuous to the discrete domain required by a computer. For the discrete version to be an accurate representation of the continuous model or the real world, extreme care must be used in selecting the spatial and temporal discretization intervals.

To demonstrate the effects of various discretization intervals, a simple program will be presented that simulates a congested bottleneck. The effects of proper and improper discretization will be shown. Two methods of reducing the excessive computing load that often accompanies dynamic simulation models will also be discussed. The first of these methods, a heuristic adaptation scheme, is used in the FRECON simulation model. Finally, the calibration and validation of the FRECON model will be presented using data from 5 days on the Santa Monica Freeway in Los Angeles.

## ORIGINS: CONTINUOUS FORMULATION

A dynamic, macroscopic model of traffic flow on a freeway may be derived from various standpoints. Payne derived the FREFLO model (formerly the MACK model) from car-following theory (2). The resulting model contains three basic equations: conservation, momentum (or dynamic), and equilibrium state. The state variables are density and speed. Phillips arrived at a similar formulation through a statistical derivation (5,6). Both models resemble the traditional hydrodynamic formulations of laminar, compressible flow.

The similarities between the Payne and Phillips dynamic equations are reassuring. The fact that two different derivations lead to the same equation terms gives one confidence in their validity. The general form of the equations will be the focus of this section, with emphasis on the overall consequences of their form.

The Payne formulation of FREFLO is contained in the following equations:

$$(\partial\rho/\partial t) + (\partial q/\partial x) = S(x,t) \tag{1}$$

$$\partial u/\partial t = [-u(\partial u/\partial x)] + [(1/c)(u_e - u)] - [b(\mu\rho/\partial x)(1/\rho)] \tag{2}$$

$$u_e = u_e(\rho) \tag{3}$$

where

$\rho(x,t)$: density at x and t,
$u(x,t)$: speed at x and t,
$q(x,t) = \rho(x,t) \cdot u(x,t)$: flow rate at x and t,
$S(x,t)$: ramp flow source term at x and t,
$u_e(\rho)$: equilibrium speed-density relation,
c: relaxation term coefficient, and
b: anticipation term coefficient.

Equation 1 represents the conservation of vehicles. The ramp source term is a static approximation of the true behavior of the ramp flows. Ramp capacity and metering rates are accounted for here. Merging effects are treated as a function of the mainline flow in the right-hand lane. The dynamics, or time change of momentum, are contained in Equation 2. The first term on the right-hand side of Equation 2 is the convection term. The second term represents the relaxation of vehicles to an equilibrium speed. This speed, in Equation 3, is experimentally determined. Figure 1 shows an equilibrium speed-density relation for the Harbor and Hollywood freeways in Los Angeles (7). The last term of Equation 2 is called an anticipation term by Payne. It represents driver response to changes in density over space.

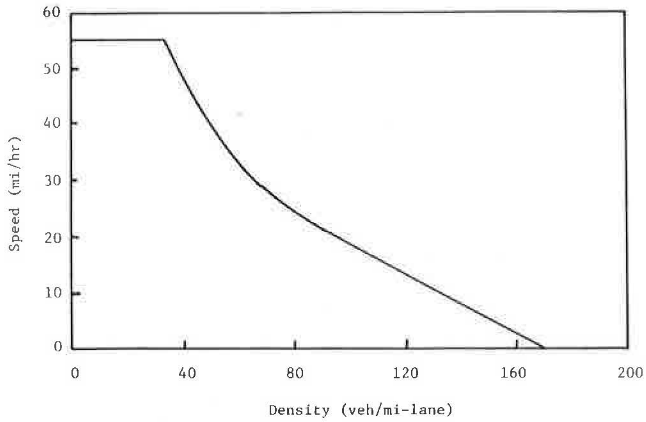


**FIGURE 1** Continuous equilibrium speed-density relation.

The coefficient in the relaxation term of Equation 2 is important in two ways. First, it is the inverse of the time constant for relaxation to the equilibrium speed. This can be observed when the traffic speed has been lowered (for example, at an incident) and then suddenly allowed to return to the speed limit. This change in speed must correspond to a realizable vehicle acceleration. Second, the only capacity information in the model is contained in the equilibrium speed-density relation. For example, short time constants force the speed to equilibrium quickly and reduce the excursions from capacity flow when high flow rates are present.

The coefficient of the anticipation term represents driver sensitivity to changes in density. This term becomes important in situations where there is a large spatial gradient in density. For example, as free-flowing vehicles approach a congested region they start to slow before they enter the congestion.

Simulation studies of simple geometries were used to tune the coefficients in the momentum equation. The primary concerns are that the resulting traffic flows show realizable accelerations, have a proper emphasis on capacity information, and behave reasonably during transients. The dynamic equation coefficients found to give the most realistic simulations for simple geometries are

$c = 0.075$ sec and
$b = 1{,}200\ (\text{mph})^2$.

These coefficients could have been set only if the model was properly discrete. In the following sections the nature of the discretization and examples of its proper and improper use will be shown.

## DISCRETE FORMULATION

Given the continuous model represented in Equations 1 and 2, how can these equations be solved in an efficient manner (i.e., on a computer)? Clearly a discrete model that is equivalent to the continuous one is required. Partial derivatives with respect to time or space would be transformed into changes over discrete steps in time or space. However, information is naturally lost during this transformation. Values previously defined over a continuum become specified only at discrete points or as averages over a region. This loss is a natural consequence of discretization but is acceptable because the resulting formulation is computer compatible. Extreme care must be taken to ensure that the resulting discrete model is a faithful representation of the continuous one and therefore can represent realistic freeway flows.

Discretization is proper when either of the following two statements is true: the discrete model must give solutions that coincide, at discrete locations, with the solutions of the continuous model; or the discrete model's solution should not be dependent on the selected discretization. These rules are used to find the maximum allowable intervals for a given model.

There is also a minimum limit on step sizes. Otherwise, the effects of machine roundoff start to cloud the solution. In the range between these two extremes (the range of proper discretization), altering the discrete steps has only a proportionate effect on the solution. In other words, step size alters only the detail of the solution.

Payne transformed the continuous formulation of FREFLO into a discrete one by defining spatially aggregated variables and then integrating each over time (2,4). Using this procedure on Equations 1 and 2 results in the following model:

$$\rho(x,t+\Delta t) = \rho(x,t) + \Delta t\left(-\{[q(x-\Delta x,t) - q(x,t)]/\Delta x\} + S(x,t)]\right) \qquad (4)$$

$$u(x,t+\Delta t) = u(x,t) + \Delta t\Big\{\{-u(x,t)\ [u(x,t) - u(x-\Delta x,t)/\Delta x]\} + \{(1/c)\ [u_e(\rho) - u(x,t)]\} - \Big(b\cdot[1/\rho(x,t)]\ \{[\rho(x + \Delta x,t) - \rho(x,t)]/\Delta x\}\Big)\Big\} \qquad (5)$$

where dx and dt have been replaced by discrete steps in space and time. The state variables are now defined only at discrete locations and times.

This system of equations could also have been derived by the explicit finite-difference method. Because the model is an explicit instead of an implicit finite-difference representation, the selection of the step sizes will affect model stability. There are two restrictions placed on the spatial and temporal step sizes. These are called the stability and accuracy limits. Because the model has two independent variables, their ratio is limited to ensure model stability. Also, both the temporal and spatial intervals must be small enough to follow all significant transitions in time and space, respectively. This limit determines the model's tracking accuracy.

The problem of stability has been discussed in the literature (3,4) and demonstrated on a simple heat transfer problem [Appendix C (1)]. The stability limit maintains causality in the flow of information down the freeway. The established stability limit for the model of Equations 4 and 5 is

$$(\Delta t/\Delta x) < 22 \text{ sec/mile} \qquad (6)$$

This stability limit applies only when the discretization intervals also satisfy the accuracy limit. The stability limit is severely reduced if the step sizes violate the accuracy requirements.

The accuracy limitation arises from the definition of a derivative and its approximations. Because the discrete model obtains its next data point by extrapolating the local slope, frequent observations of this slope are needed when it changes abruptly in time or space. Let us examine the anticipation term of Equation 2:

$$b(\partial\rho/\partial x)\ (1/\rho) \qquad (7)$$

This term uses information on the local slope of the density with respect to space.

Figure 2 shows a simulated density profile of congestion resulting from a lane drop at x = 0.5 mile. For the discrete model to follow this contour the spatial discretization must be small enough to ensure that the spatial slope of the density has not changed appreciably over each step. Spatial step sizes similar to the extent of the shock front at x = 0.25 are required to ensure that the entire region of congestion is modeled accurately.

The proper value for the stability and accuracy limits can be found experimentally. A properly discrete model is one with simulation results that are independent of the step sizes used. Therefore, the discretization limits can be found by repeated simulations with various step sizes. This process is discussed in the following section.

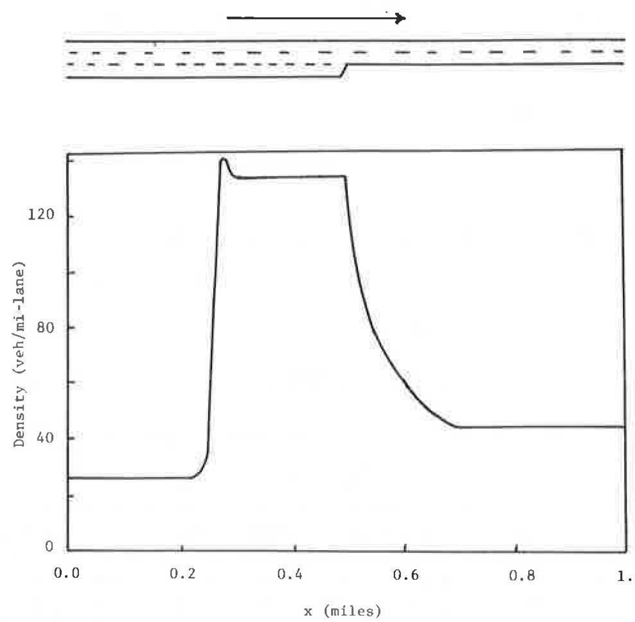


**FIGURE 2 Density contour at lane drop.**

## EFFECTS OF DISCRETIZATION

To show the consequences of proper and improper discretization more concretely, the simple geometry of a lane drop with a constant input flow (Figure 3) is used. In this example the lane capacity is set to 2,000 vehicles per hour and the input demand is 4,500 vehicles per hour. It is expected that this demand level would cause capacity flow in subsections 6 through 10 and queueing on the subsections upstream of subsection 6.

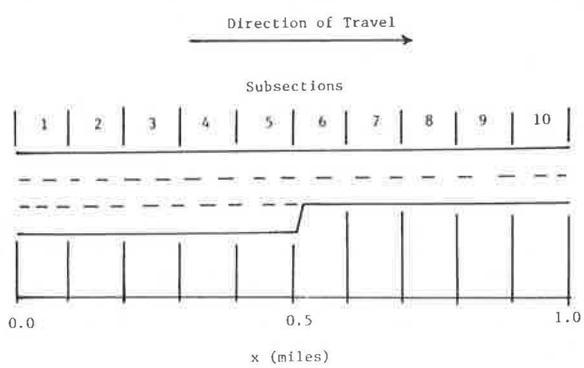


**FIGURE 3 Lane drop geometry.**

The model represented in Equations 4 and 5 and Figure 1 has been coded into a simple FORTRAN program (Table 1). To maintain simplicity in this program all inputs are assigned statements and the output is printed at each time step. Although this program is used to present simulations of the geometry of Figure 3, the output has been processed here into a more readable format. For the following procedures, the model generates instantaneous speeds and densities averaged over each subsection and the instantaneous flow leaving each subsection.

To demonstrate the effects of various discretization intervals the program is used to simulate a 10-min period of the bottleneck geometry of Figure 3. The spatial steps in the model are arbitrarily set equal to the subsection lengths (0.1 mile) and the temporal steps are set to satisfy the stability criterion (Equation 6). The results (Figure 4 and Table 2) show that the capacity of the bottleneck is exceeded and the highest densities (more than 100 vehicles per mile-lane) are inside the bottleneck. This is similar to a simulation presented in the literature (4).

Clearly this is not the expected behavior for an overloaded bottleneck. The first aspect to be investigated is whether the stability limit is valid for this spatial discretization. Dividing the time steps by two gives the simulation shown in Figure 5 and Table 3. Although this result is quite different from that of the previous simulation, it is no more real because the bottleneck flows are less than 35 percent of capacity. Further reductions of the time step do not alter the result. Therefore, the stability limit for this spatial step is in fact less than the prescribed stability limit.

To get a more realistic simulation the equilibrium speed-density relation could be artificially altered as has been suggested in the literature (3,4). It is recommended instead that an investigation of the spatial accuracy limit be performed. In Figures 6-9 and Tables 4-7 results with spatial step sizes set at 0.05, 0.02, 0.01, and 0.005 mile, respectively, are presented. The time steps used were also reduced in each case to satisfy the stability limit. For convenience the model output is still presented as averaged speed and densities over each of the ten original subsections. However, now each of these subsections is comprised of subdivisions (the spatial steps used in the program). The flow rate still represents the flow leaving each subsection.

The solution changes dramatically as each subsection is divided into smaller pieces. This evolution approaches a limit when the subsection size is 0.01 mile (52 ft). Further reduction in the step sizes does not alter the nature of the simulation result, only the detail observed in the transition regions. This experiment may be duplicated by altering the number of subsections (nsect), length of the subsections (x), and the time step (delt) in the FORTRAN program (Table 1).

In the final simulations (Figures 8 and 9 and Tables 6 and 7) the bottleneck capacity is adhered to and the bottleneck densities are typical for capacity flow. There is queueing on subsections upstream of the lane drop and an acceleration region exists in subsection 6. It should be emphasized that the only difference between the simulation of Figure 4 and Table 2 and that of Figures 8 and 9 and Tables 6 and 7 is in the length of the spatial discretization (and the associated temporal steps needed for stability). As the model becomes more properly dis-

**TABLE 1 FORTRAN Program for Lane Drop Simulation**

```
C       SIMPLE FREEWAY SIMULATION MODEL
        dimension x(200),lanes(200),u(200),rho(200),vol(200)
C       NUMBER OF SUBSECTIONS (FIRST, LAST ARE BOUNDARY CONDITIONS)
        nsect = 12
C       SET INITIAL CONDITIONS AND LANE NUMBERS
        do 10 i=1,nsect/2
         lanes(i) = 3
         rho(i) = 27.
   10    u(i) = 55.
        do 20 i=(nsect/2)+1,nsect
         lanes(i) = 2
         rho(i) = 50.
   20    u(i) = 40.
C       SET LENGTH OF SUBDIVISIONS AND INITIAL FLOWS
        do 30 i=1,nsect
         x(i) = 0.1
   30    vol(i+1) = rho(i)*u(i)
C       SET COEFFICIENTS, INPUT FLOW, TIME STEP, AND STOP TIME
        c = 0.075/3600.
        b = 1200.
        vol(1) = 4500.
        delt = 1.0/3600.
        tstop = 600./3600.
C
   40   continue
C       CALCULATE NEXT SPEED AND FLOW FOR EACH SUBDIVISION
        u(1) = u(2)
        vol(2) = rho(1)*u(1)
        do 50 i=nsect-1,2,-1
         vol(i+1) = rho(i)*u(i)
   50    u(i) = u(i) - delt * ( u(i)*2.*(u(i)-u(i-1))/
    1      (x(i)+x(i-1)) + (u(i)-ue(rho(i),i,nsect))/c +
    2      b*2.*(rho(i+1)-rho(i))/(rho(i)*(x(i+1)+x(i))) )
C       CALCULATE NEXT DENSITY FOR EACH SUBDIVISION
        rho(1) = rho(1) + delt*(vol(1)-lanes(1)*vol(2))/lanes(1)
        do 70 i=2,nsect-1
   70    rho(i) = rho(i) + delt * ( vol(i)*lanes(i-1) -
    1      vol(i+1)*lanes(i))/(x(i)*lanes(i))
        rho(nsect) = rho(nsect-1)
C       UPDATE TIME AND PRINT CURRENT STATES
        time = time + delt
        timsec = time*3600.
        write (6,90) (timsec,i,u(i),rho(i),vol(i+1),i=2,nsect-1)
   90   format (5x,f7.1,i6,3f10.2)
        if (time.lt.tstop) go to 40
        stop
        end
C
C
C     EQUILIBRIUM SPEED-DENSITY RELATION
      function ue(rho,i,nsect)
      d = rho
      if (rho.gt.100) d = 100.
      ue = ((-7.4e-5*d+0.0215)*d-2.31)*d+107.
      if (rho.gt.100.) ue = ue - ((rho-100.)*ue/70.)
C     SET CAPACITY AT 2000.
      ue = ue * (2000./1800.)
C     FOLLOWING LINE USED FOR DISCONTINUOUS RELATION
C     if (rho.gt.60.) ue = ue * 0.8
      if (ue.gt.55.) ue = 55.
      if (ue.lt.0.) ue = 0.
      return
      end
```

```
Time                          Subsection
(min)   1     2     3     4     5     6     7     8     9     10

  0.                               00000000000000000000000000000000000000000000000000
  1.                               IIIIIIIIIIIIIIIIIIII0000000000IIIIIIIIII0000000000
  2.                               IIIIIIIIII$$$$$$$$$$0000000000$$$$$$$$$$0000000000
  3.                               IIIIIIIIII$$$$$$$$$$0000000000$$$$$$$$$$0000000000
  4.                               IIIIIIIIII$$$$$$$$$$0000000000$$$$$$$$$$0000000000
  5.                               IIIIIIIIII$$$$$$$$$$0000000000$$$$$$$$$$0000000000
  6.                               IIIIIIIIII$$$$$$$$$$0000000000$$$$$$$$$$0000000000
  7.                               IIIIIIIIII$$$$$$$$$$0000000000$$$$$$$$$$0000000000
  8.                               IIIIIIIIII$$$$$$$$$$0000000000$$$$$$$$$$0000000000
  9.                               IIIIIIIIII$$$$$$$$$$0000000000$$$$$$$$$$0000000000
 10.                               IIIIIIIIII$$$$$$$$$$0000000000$$$$$$$$$$0000000000

        1     2     3     4     5     6     7     8     9     10
```

Legend For Contour Map

| Lower Limit | Upper Limit | Symbol |
|---|---|---|
| 0. | 40. | |
| 40. | 50. | . |
| 50. | 60. | O |
| 60. | 80. | I |
| 80. | 120. | $ |
| 120. | 1000. | # |

**FIGURE 4 Unstable subsection averaged density (vehicles/mile-lane)—continuous equilibrium relation with $\Delta x = 0.1$ mile.**

**TABLE 2 Unstable Volume Leaving Subsections (Vehicles/Hour)—Continuous Equilibrium Relation with $\Delta x$ = 0.1 Mile**

| Time (min) | Subsection Number 1 | 2 | 3 | 4 | 5 | 6 | 7 | 8 | 9 | 10 |
|---|---|---|---|---|---|---|---|---|---|---|
| 0 | 4455 | 4455 | 4455 | 4455 | 4455 | 4000 | 4000 | 4000 | 4000 | 4000 |
| 1 | 4468 | 4465 | 4463 | 4458 | 4410 | 4203 | 3848 | 3811 | 3533 | 3506 |
| 2 | 4487 | 4486 | 4484 | 4482 | 4479 | 4472 | 4448 | 4408 | 4313 | 4314 |
| 3 | 4495 | 4494 | 4494 | 4493 | 4492 | 4490 | 4488 | 4485 | 4478 | 4416 |
| 4 | 4498 | 4498 | 4497 | 4497 | 4497 | 4496 | 4495 | 4494 | 4493 | 4561 |
| 5 | 4499 | 4499 | 4499 | 4499 | 4499 | 4499 | 4498 | 4498 | 4497 | 4427 |
| 6 | 4500 | 4500 | 4500 | 4500 | 4500 | 4499 | 4499 | 4499 | 4499 | 4569 |
| 7 | 4500 | 4500 | 4500 | 4500 | 4500 | 4500 | 4500 | 4500 | 4500 | 4429 |
| 8 | 4500 | 4500 | 4500 | 4500 | 4500 | 4500 | 4500 | 4500 | 4500 | 4570 |
| 9 | 4500 | 4500 | 4500 | 4500 | 4500 | 4500 | 4500 | 4500 | 4500 | 4430 |
| 10 | 4500 | 4500 | 4500 | 4500 | 4500 | 4500 | 4500 | 4500 | 4500 | 4570 |

**TABLE 3 Volume Leaving Subsections (Vehicles/Hour)—Continuous Equilibrium Relation with $\Delta x$ = 0.1 Mile**

| Time (min) | Subsection Number 1 | 2 | 3 | 4 | 5 | 6 | 7 | 8 | 9 | 10 |
|---|---|---|---|---|---|---|---|---|---|---|
| 0 | 4455 | 4455 | 4455 | 4455 | 4455 | 4000 | 4000 | 4000 | 4000 | 4000 |
| 1 | 4468 | 4465 | 4463 | 4460 | 4436 | 4168 | 4065 | 3708 | 3893 | 3567 |
| 2 | 4487 | 4486 | 4484 | 4482 | 4462 | 4167 | 3893 | 4126 | 3576 | 3978 |
| 3 | 4495 | 4494 | 4494 | 4492 | 4454 | 3640 | 3884 | 3828 | 4148 | 4002 |
| 4 | 4498 | 4498 | 4497 | 4485 | 4112 | 1430 | 1940 | 2509 | 3004 | 3759 |
| 5 | 4499 | 4499 | 4498 | 4458 | 3367 | 2176 | 2134 | 2056 | 2005 | 1962 |
| 6 | 4500 | 4499 | 4493 | 4301 | 514 | 2066 | 2116 | 2184 | 2212 | 2235 |
| 7 | 4500 | 4499 | 4467 | 3578 | 755 | 1492 | 1548 | 1580 | 1610 | 1699 |
| 8 | 4499 | 4496 | 4382 | 1281 | 1468 | 1423 | 1411 | 1424 | 1421 | 1426 |
| 9 | 4496 | 4474 | 3780 | 59 | 1112 | 1379 | 1400 | 1396 | 1407 | 1413 |
| 10 | 4484 | 4394 | 1748 | 843 | 1029 | 1266 | 1269 | 1293 | 1302 | 1315 |

```
Time                           Subsection
(min)    1         2         3         4         5         6         7         8         9        10
     ----+---------+---------+---------+---------+---------+---------+---------+---------+---------+
  0.                                                  OOOOOOOOOOOOOOOOOOOOOOOOOOOOOOOOOOOOOOOOOOOOOOOOOO
  1.                                                  IIIIIIIIIIIIIIIIIIIIIIIIIIIIIIOOOOOOOOOOOOOOOOOOOO
  2.                                                  $$$$$$$$$$$$$$$$$$$$IIIIIIIIIIIIIIIIIIIIOOOOOOOOOO
  3.                                                  ##########IIIIIIIIIIIIIIIIIIIIIIIIIIIIIIOOOOOOOOOO
  4.                                        OOOOOOOOOO##########
  5.                                        $$$$$$$$$$##########
  6.                              ..........####################
  7.                              $$$$$$$$$$####################
  8.                              ##############################
  9.                    IIIIIIIIII##############################
 10.                    ########################################
     ----+---------+---------+---------+---------+---------+---------+---------+---------+---------+
         1         2         3         4         5         6         7         8         9        10
```

Legend For Contour Map

| Lower Limit | Upper Limit | Symbol |
|---|---|---|
| 0. | 40. | |
| 40. | 50. | . |
| 50. | 60. | O |
| 60. | 80. | I |
| 80. | 120. | $ |
| 120. | 1000. | # |

**FIGURE 5 Subsection averaged density (vehicles/mile-lane)—continuous equilibrium relation with $\Delta x$ = 0.1 mile.**

```
Time                           Subsection
(min)    1         2         3         4         5         6         7         8         9        10
     ----+---------+---------+---------+---------+---------+---------+---------+---------+---------+
  0.                                                  OOOOOOOOOOOOOOOOOOOOOOOOOOOOOOOOOOOOOOOOOOOOOOOOOO
  1.                                                  IIIIIIIIIIOOOOOOOOOO....................OOOOOOOOOO
  2.                                                  $$$$$$$$$$IIIIIIIIII..............................
  3.                                        IIIIIIIIII##########                    ....................
  4.                                        ##########$$$$$$$$$$
  5.                              ####################IIIIIIIIII
  6.                    IIIIIIIIII####################OOOOOOOOOO
  7.                    ####################..........OOOOOOOOOO
  8.          ####################$$$$$$$$$$
  9.     IIIIIIIIII####################
 10.     ####################$$$$$$$$$$                    OOOOOOOOOO..........
     ----+---------+---------+---------+---------+---------+---------+---------+---------+---------+
         1         2         3         4         5         6         7         8         9        10
```

Legend For Contour Map

| Lower Limit | Upper Limit | Symbol |
|---|---|---|
| 0. | 40. | |
| 40. | 50. | . |
| 50. | 60. | O |
| 60. | 80. | I |
| 80. | 120. | $ |
| 120. | 1000. | # |

**FIGURE 6 Subsection averaged density (vehicles/mile-lane)—continuous equilibrium relation with $\Delta x$ = 0.05 mile.**

```
Time                               Subsection
(min)     1         2         3         4         5         6         7         8         9        10
  0.                                                  00000000000000000000000000000000000000000000000000
  1.                                                  $$$$$$$$$$0000000000..........0000000000..........
  2.                                        IIIIIIIIII00000000000000000000....................0000000000
  3.                                        $$$$$$$$$$IIIIIIIIII..............................0000000000
  4.                                        ##########0000000000          ..............................
  5.                              IIIIIIIIII$$$$$$$$$$IIIIIIIIII                    ..........0000000000
  6.                              ##########$$$$$$$$$$0000000000                              ..........
  7.                    0000000000##############################IIIIIIIIII
  8.                    $$$$$$$$$$$$$$$$$$$$$$$$$$$$$$IIIIIIIIII
  9.                    $$$$$$$$$$####################IIIIIIIIII
 10.          $$$$$$$$$$$$$$$$$$$$$$$$$$$$$$$$$$$$$$$$$$$$$$$$$$
          1         2         3         4         5         6         7         8         9        10
```

Legend For Contour Map

| Lower Limit | Upper Limit | Symbol |
|---|---|---|
| 0. | 40. | |
| 40. | 50. | . |
| 50. | 60. | 0 |
| 60. | 80. | I |
| 80. | 120. | $ |
| 120. | 1000. | # |

**FIGURE 7** Subsection averaged density (vehicles/mile-lane)—continuous equilibrium relation with $\Delta x = 0.02$ mile.

```
Time                               Subsection
(min)     1         2         3         4         5         6         7         8         9        10
  0.                                                  00000000000000000000000000000000000000000000000000
  1.                                                  $$$$$$$$$$..........0000000000....................
  2.                                        IIIIIIIIIIIIIIIIIIII0000000000..........0000000000..........
  3.                                        $$$$$$$$$$IIIIIIIIII0000000000....................0000000000
  4.                                        $$$$$$$$$$IIIIIIIIII0000000000....................0000000000
  5.                              ..........##########IIIIIIIIII0000000000....................0000000000
  6.                              IIIIIIIIII##########IIIIIIIIII0000000000..............................
  7.                              $$$$$$$$$$##########IIIIIIIIII0000000000..............................
  8.                              ####################IIIIIIIIII0000000000..............................
  9.                    0000000000####################IIIIIIIIII0000000000..............................
 10.                    $$$$$$$$$$####################IIIIIIIIII0000000000..............................
          1         2         3         4         5         6         7         8         9        10
```

Legend For Contour Map

| Lower Limit | Upper Limit | Symbol |
|---|---|---|
| 0. | 40. | |
| 40. | 50. | . |
| 50. | 60. | 0 |
| 60. | 80. | I |
| 80. | 120. | $ |
| 120. | 1000. | # |

**FIGURE 8** Subsection averaged density (vehicles/mile-lane)—continuous equilibrium relation with $\Delta x = 0.01$ mile.

```
Time                               Subsection
(min)     1         2         3         4         5         6         7         8         9        10
  0.                                                  00000000000000000000000000000000000000000000000000
  1.                                                  IIIIIIIIII..........0000000000....................
  2.                                        IIIIIIIIII$$$$$$$$$$..............................0000000000
  3.                                        $$$$$$$$$$$$$$$$$$$$0000000000..........0000000000..........
  4.                                        $$$$$$$$$$$$$$$$$$$$0000000000..........0000000000..........
  5.                                        ##########$$$$$$$$$$0000000000....................0000000000
  6.                              IIIIIIIIII##########$$$$$$$$$$0000000000....................0000000000
  7.                              $$$$$$$$$$##########$$$$$$$$$$0000000000....................0000000000
  8.                              ####################$$$$$$$$$$0000000000....................0000000000
  9.                    ..........####################$$$$$$$$$$0000000000....................0000000000
 10.                    IIIIIIIIII####################$$$$$$$$$$0000000000..............................
          1         2         3         4         5         6         7         8         9        10
```

Legend For Contour Map

| Lower Limit | Upper Limit | Symbol |
|---|---|---|
| 0. | 40. | |
| 40. | 50. | . |
| 50. | 60. | 0 |
| 60. | 80. | I |
| 80. | 120. | $ |
| 120. | 1000. | # |

**FIGURE 9** Subsection averaged density (vehicles/mile-lane)—continuous equilibrium relation with $\Delta x =$ 0.005 mile.

**TABLE 4 Volume Leaving Subsections (Vehicles/Hour)—Continuous Equilibrium Relation with $\Delta x$ = 0.05 Mile**

| Time (min) | Subsection Number 1 | 2 | 3 | 4 | 5 | 6 | 7 | 8 | 9 | 10 |
|---|---|---|---|---|---|---|---|---|---|---|
| 0 | 4455 | 4455 | 4455 | 4455 | 4455 | 4000 | 4000 | 4000 | 4000 | 4000 |
| 1 | 4468 | 4465 | 4463 | 4461 | 4431 | 4085 | 3971 | 3988 | 4001 | 4001 |
| 2 | 4487 | 4486 | 4484 | 4483 | 4456 | 4056 | 3950 | 3953 | 3994 | 4009 |
| 3 | 4495 | 4495 | 4494 | 4490 | 3768 | 3122 | 3640 | 3903 | 3975 | 4010 |
| 4 | 4498 | 4498 | 4497 | 4428 | 1420 | 2102 | 2211 | 2338 | 2623 | 2970 |
| 5 | 4499 | 4499 | 4486 | 2189 | 1436 | 1880 | 1761 | 1714 | 1712 | 1733 |
| 6 | 4500 | 4497 | 3809 | 773 | 2946 | 3126 | 3058 | 2974 | 2889 | 2786 |
| 7 | 4499 | 4381 | 490 | 1625 | 3732 | 3727 | 3686 | 3622 | 3520 | 3396 |
| 8 | 4471 | 1568 | 898 | 3624 | 3863 | 3791 | 3767 | 3748 | 3731 | 3725 |
| 9 | 3398 | 499 | 1979 | 3691 | 3788 | 3804 | 3779 | 3775 | 3769 | 3772 |
| 10 | 106 | 1125 | 3653 | 3697 | 3747 | 3808 | 3784 | 3780 | 3777 | 3777 |

**TABLE 5 Volume Leaving Subsections (Vehicles/Hour)—Continuous Equilibrium Relation with $\Delta x$ = 0.02 Mile**

| Time (min) | Subsection Number 1 | 2 | 3 | 4 | 5 | 6 | 7 | 8 | 9 | 10 |
|---|---|---|---|---|---|---|---|---|---|---|
| 0 | 4455 | 4455 | 4455 | 4455 | 4455 | 4000 | 4000 | 4000 | 4000 | 4000 |
| 1 | 4468 | 4465 | 4463 | 4461 | 4431 | 3995 | 3978 | 4005 | 4000 | 4000 |
| 2 | 4487 | 4486 | 4485 | 4483 | 3626 | 3986 | 3950 | 3990 | 4011 | 3995 |
| 3 | 4495 | 4495 | 4494 | 4491 | 4062 | 3890 | 4015 | 3960 | 4004 | 3997 |
| 4 | 4498 | 4498 | 4498 | 4402 | 3761 | 3874 | 3949 | 4021 | 3975 | 4019 |
| 5 | 4499 | 4499 | 4499 | 3610 | 4052 | 3852 | 3859 | 3937 | 4032 | 3980 |
| 6 | 4500 | 4500 | 4493 | 3672 | 3530 | 3859 | 3845 | 3861 | 3915 | 4041 |
| 7 | 4500 | 4500 | 4014 | 4227 | 4067 | 3836 | 3862 | 3843 | 3858 | 3903 |
| 8 | 4500 | 4499 | 3446 | 3408 | 3747 | 3862 | 3837 | 3856 | 3845 | 3854 |
| 9 | 4500 | 4297 | 4286 | 4182 | 3854 | 3837 | 3857 | 3843 | 3852 | 3846 |
| 10 | 4500 | 3387 | 3450 | 3679 | 4069 | 3853 | 3846 | 3852 | 3845 | 3851 |

crete in space, the stability limit gradually increases to the value in Equation 6. This property can be confirmed by altering the value of the time step (delt) in the FORTRAN program (Table 1).

It is not surprising that simulation accuracy is dependent on the length of the spatial steps. As discussed earlier, spatial steps on the order of 0.01 mile would be needed to follow the changing slope near the queueing shock front. Use of larger intervals where the slope is changing leads to erroneous solutions that have no relation to the continuous formulation nor bear any resemblance to freeway behavior.

The spatial steps required by the model are a result of the form of the differential terms in the system equations and the model parameters. It has been found that these limits are quite insensitive to the shape of the equilibrium speed-density relation. For example, consider the alteration of the equilibrium speed-density relation shown in Figure 10. Ceder (8) has found that traffic flow may be better approximated by discontinuous, multiregime curves of this type.

Figure 11 and Table 8 show a simulation using this curve and spatial steps of 0.1 mile. The solu-

**TABLE 6 Volume Leaving Subsections (Vehicles/Hour)—Continuous Equilibrium Relation with $\Delta x$ = 0.01 Mile**

| Time (min) | Subsection Number 1 | 2 | 3 | 4 | 5 | 6 | 7 | 8 | 9 | 10 |
|---|---|---|---|---|---|---|---|---|---|---|
| 0 | 4455 | 4455 | 4455 | 4455 | 4455 | 4000 | 4000 | 4000 | 4000 | 4000 |
| 1 | 4468 | 4465 | 4463 | 4461 | 4368 | 3971 | 4000 | 4000 | 3999 | 4000 |
| 2 | 4487 | 4486 | 4485 | 4483 | 3942 | 3986 | 3953 | 4023 | 3991 | 4001 |
| 3 | 4495 | 4495 | 4494 | 4493 | 3974 | 3977 | 3968 | 3969 | 4016 | 3990 |
| 4 | 4498 | 4498 | 4498 | 4490 | 3973 | 3975 | 3975 | 3967 | 4020 | 3966 |
| 5 | 4499 | 4499 | 4499 | 4218 | 3974 | 3975 | 3975 | 3974 | 3979 | 3985 |
| 6 | 4500 | 4500 | 4500 | 3960 | 3975 | 3975 | 3975 | 3975 | 3975 | 4028 |
| 7 | 4500 | 4500 | 4500 | 3975 | 3975 | 3975 | 3975 | 3975 | 3975 | 4001 |
| 8 | 4500 | 4500 | 4459 | 3975 | 3975 | 3975 | 3975 | 3975 | 3974 | 3977 |
| 9 | 4500 | 4500 | 4041 | 3974 | 3975 | 3975 | 3975 | 3975 | 3975 | 3975 |
| 10 | 4500 | 4500 | 3977 | 3975 | 3975 | 3975 | 3975 | 3975 | 3975 | 3975 |

**TABLE 7 Volume Leaving Subsections (Vehicles/Hour)—Continuous Equilibrium Relation with $\Delta x$ = 0.005 Mile**

| Time (min) | Subsection Number 1 | 2 | 3 | 4 | 5 | 6 | 7 | 8 | 9 | 10 |
|---|---|---|---|---|---|---|---|---|---|---|
| 0 | 4455 | 4455 | 4455 | 4455 | 4455 | 4000 | 4000 | 4000 | 4000 | 4000 |
| 1 | 4468 | 4465 | 4463 | 4461 | 4258 | 3969 | 4008 | 3999 | 4000 | 4000 |
| 2 | 4487 | 4486 | 4485 | 4483 | 4050 | 3981 | 3971 | 3995 | 4004 | 4000 |
| 3 | 4495 | 4495 | 4494 | 4493 | 4012 | 3988 | 3955 | 4026 | 3967 | 4003 |
| 4 | 4498 | 4498 | 4498 | 4496 | 4000 | 3987 | 3967 | 3955 | 3989 | 3982 |
| 5 | 4499 | 4499 | 4499 | 4270 | 3993 | 3986 | 3973 | 3963 | 4036 | 3937 |
| 6 | 4500 | 4500 | 4500 | 3996 | 3989 | 3985 | 3977 | 3970 | 3991 | 3959 |
| 7 | 4500 | 4500 | 4500 | 3987 | 3987 | 3984 | 3979 | 3974 | 3971 | 3963 |
| 8 | 4500 | 4500 | 4492 | 3986 | 3985 | 3984 | 3980 | 3977 | 3973 | 3959 |
| 9 | 4500 | 4500 | 4135 | 3984 | 3984 | 3983 | 3981 | 3978 | 3976 | 3969 |
| 10 | 4500 | 4500 | 3985 | 3984 | 3984 | 3983 | 3981 | 3980 | 3977 | 4025 |

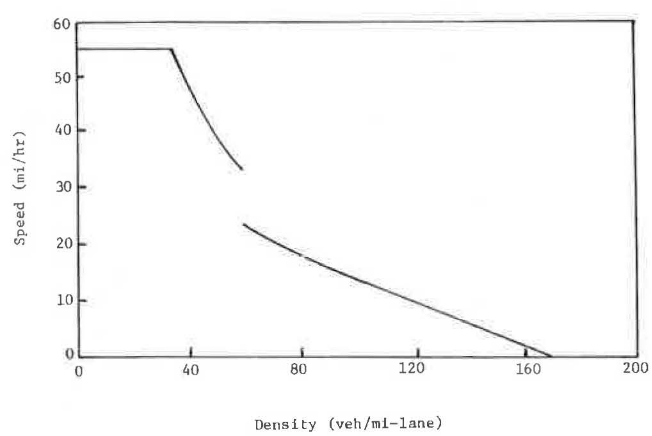


FIGURE 10 Discontinuous equilibrium speed-density relation.

tions evolve toward the simulation result shown in Figure 12 and Table 9. Here the spatial steps are 0.01 mile. Further reduction of the step sizes does not significantly alter the result. This process can

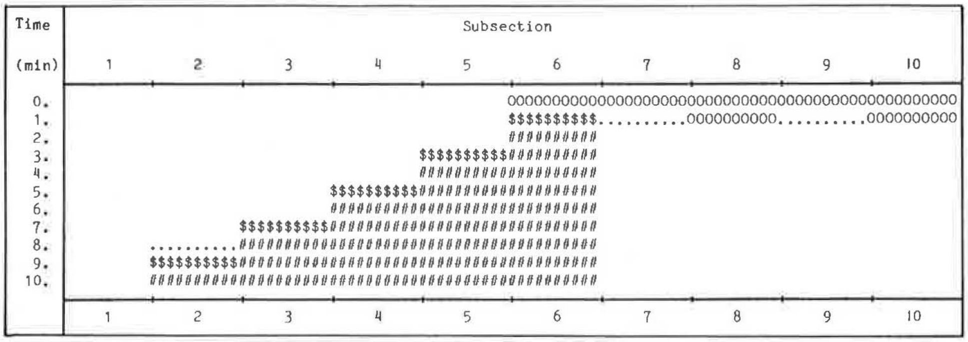

Legend For Contour Map

| Lower Limit | Upper Limit | Symbol |
|---|---|---|
| 0. | 40. | |
| 40. | 50. | . |
| 50. | 60. | O |
| 60. | 80. | I |
| 80. | 120. | $ |
| 120. | 1000. | # |

FIGURE 11 Subsection averaged density (vehicles/mile-lane)—discontinuous equilibrium relation with $\Delta x = 0.1$ mile.

**TABLE 8 Volume Leaving Subsections (Vehicles/Hour)—Discontinuous Equilibrium Relation with $\Delta x = 0.1$ Mile**

| Time | Subsection Number | | | | | | | | | |
|---|---|---|---|---|---|---|---|---|---|---|
| (min) | 1 | 2 | 3 | 4 | 5 | 6 | 7 | 8 | 9 | 10 |
| 0 | 4455 | 4455 | 4455 | 4455 | 4455 | 4000 | 4000 | 4000 | 4000 | 4000 |
| 1 | 4468 | 4465 | 4463 | 4459 | 4418 | 3836 | 3901 | 3743 | 3897 | 3562 |
| 2 | 4487 | 4486 | 4484 | 4478 | 4352 | 2201 | 2521 | 3137 | 3410 | 3829 |
| 3 | 4495 | 4494 | 4493 | 4462 | 3555 | 1840 | 1766 | 1679 | 1663 | 1782 |
| 4 | 4498 | 4498 | 4493 | 4348 | 828 | 1890 | 1921 | 1969 | 1981 | 1986 |
| 5 | 4499 | 4498 | 4465 | 3484 | 669 | 1386 | 1439 | 1470 | 1526 | 1581 |
| 6 | 4499 | 4494 | 4329 | 603 | 1201 | 1293 | 1287 | 1304 | 1305 | 1313 |
| 7 | 4495 | 4454 | 3223 | 270 | 944 | 1214 | 1235 | 1235 | 1248 | 1257 |
| 8 | 4467 | 4266 | 292 | 724 | 942 | 1121 | 1122 | 1142 | 1148 | 1159 |
| 9 | 4300 | 2882 | 156 | 595 | 920 | 1061 | 1076 | 1072 | 1081 | 1087 |
| 10 | 3613 | 172 | 488 | 624 | 880 | 1007 | 1006 | 1021 | 1025 | 1031 |

**TABLE 9 Volume Leaving Subsections (Vehicles/Hour)—Discontinuous Equilibrium Relation with $\Delta x = 0.01$ Mile**

| Time | Subsection Number | | | | | | | | | |
|---|---|---|---|---|---|---|---|---|---|---|
| (min) | 1 | 2 | 3 | 4 | 5 | 6 | 7 | 8 | 9 | 10 |
| 0 | 4455 | 4455 | 4455 | 4455 | 4455 | 4000 | 4000 | 4000 | 4000 | 4000 |
| 1 | 4468 | 4465 | 4463 | 4461 | 3896 | 3811 | 4012 | 3997 | 4000 | 4000 |
| 2 | 4487 | 4486 | 4485 | 4481 | 3576 | 3581 | 3589 | 3814 | 4011 | 4002 |
| 3 | 4495 | 4495 | 4494 | 3888 | 3580 | 3580 | 3580 | 3580 | 3589 | 3804 |
| 4 | 4498 | 4498 | 4495 | 3578 | 3580 | 3580 | 3580 | 3580 | 3580 | 3580 |
| 5 | 4499 | 4499 | 3879 | 3580 | 3580 | 3580 | 3580 | 3580 | 3580 | 3580 |
| 6 | 4500 | 4494 | 3579 | 3580 | 3580 | 3580 | 3580 | 3580 | 3580 | 3580 |
| 7 | 4500 | 3827 | 3580 | 3580 | 3580 | 3580 | 3580 | 3580 | 3580 | 3580 |
| 8 | 4490 | 3580 | 3580 | 3580 | 3580 | 3580 | 3580 | 3580 | 3580 | 3580 |
| 9 | 3771 | 3580 | 3580 | 3580 | 3580 | 3580 | 3580 | 3580 | 3580 | 3580 |
| 10 | 3580 | 3580 | 3580 | 3580 | 3580 | 3580 | 3580 | 3580 | 3580 | 3580 |

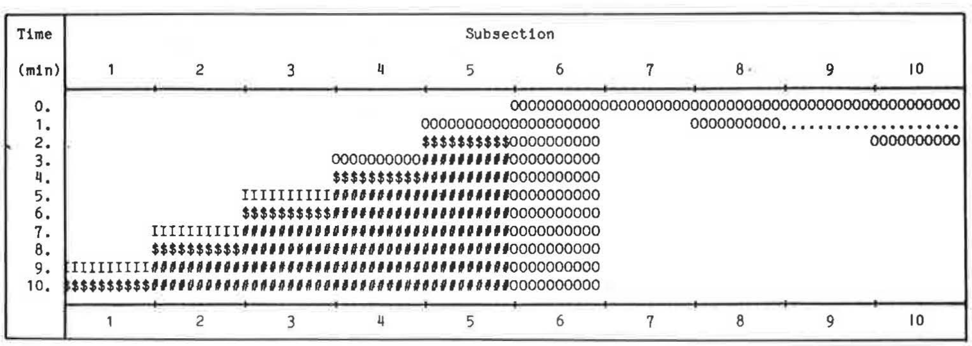

Legend For Contour Map

| Lower Limit | Upper Limit | Symbol |
|---|---|---|
| 0. | 40. | |
| 40. | 50. | . |
| 50. | 60. | O |
| 60. | 80. | I |
| 80. | 120. | $ |
| 120. | 1000. | # |

FIGURE 12 Subsection averaged density (vehicles/mile-lane)—discontinuous equilibrium relation with $\Delta x = 0.01$ mile.

be duplicated by activating the commented "if" statement in the FORTRAN program (Table 1).

One curious result of this simulation is that the bottleneck is not filled to capacity. This is due to the upstream congested region reaching equilibrium on the discontinuous curve of Figure 10. This equilibrium cannot simultaneously satisfy continuity at the lane drop and provide flows high enough to fill the bottleneck. This situation may not occur in real traffic because the equilibrium relation used here was not derived from traffic data. However, the discretization limits remained the same in the face of these very different traffic flows.

With spatial step sizes of 0.01 mile required to follow changes in the density-space slope, the possibility of unmanageable input and output arises. This is avoided by permitting the user to use standard subsections to define the freeway geometry and demands. These subsections are related to physical divisions and have no direct bearing on the required mathematical discretization. The model internally divides each subsection into the necessary subdivisions so that model accuracy is maintained. The results are printed out as subsection values to keep the output readable.

A further difficulty that arises from the use of proper discretization is that of computing time. Consider a simulation of the Santa Monica Freeway in Los Angeles. The site is 7.7 miles long and a 3-hr period is to be simulated. The use of spatial steps of 0.01 mile and their associated temporal steps of 0.2 sec results in 770 subdivisions requiring 54,000 time steps to complete the simulation. This process would use 40 central processing unit (CPU) hours of computing time on a DEC VAX11/750. It would be advantageous to find a way of reducing this computing time while still maintaining the discrete model's integrity.

## HEURISTIC SCHEME FOR ADAPTING THE DISCRETIZATION

Although the use of very small spatial steps is required to maintain the model's accuracy, these steps are not required at all times and at all locations during a simulation. This idea motivates the use of an adaptive scheme. The term that most restricts the maximum spatial step needed is the anticipation term (Equation 7). It implies that small steps are required to follow the changing density-space slope. Further, this process will become more critical at higher densities. It is possible to exploit some of the freeway flow properties to develop a heuristic scheme for placing subdivisions within the subsections only where and when they are required to maintain the model's accuracy. This adaptive scheme is at the heart of the FRECON model.

Consider again the contour of density for the congested bottleneck (Figure 2). In the region from $x = 0.0$ to $0.25$, large subdivisions could be used because the density is low and the slope is constant. The shock front at $x = 0.25$ requires very short steps because the slope changes abruptly. The queued region ($x = 0.3$ to $0.5$) also needs short divisions because the density is large. The acceleration region ($x = 0.5$ to $0.7$) has a changing slope so it too requires small subdivisions. The capacity flow area ($x = 0.7$ to $1.0$) needs only moderate sized subdivisions because of its density level.

Similar examinations can be made of other simple geometries. In general, all freeway situations can be divided into the following classes: lane drop (or heavy on-ramp), lane add (or heavy off-ramp), capacity flow, queued flow, and incident. Each has a pattern of maximum subdivision lengths associated with it. These are required when the flow rises above a given threshold inducing sharp gradients in the density-space profile. Therefore, it is possible to select the subdivision pattern by examining the geometry and the current flow level. When all the patterns for a given time period have been established, they are placed on the freeway to provide the needed spatial discretization.

This process is repeated at regular, user-set intervals (a typical value is every minute) so that the freeway is always properly, but not excessively, subdivided. In cases where the input demands vary at a higher frequency, the adaptation of the subdivisions can be performed at a comparable frequency or a worst-case can be assumed and the adaptation can take place at a lower frequency.

Each time the subdivision patterns are laid down on the freeway subsections, care must be taken that the original geometry is not altered. Also, in regions where the subdivision patterns overlap, the limiting step sizes (i.e., the smallest of the steps) must be maintained. Each time new patterns replace old patterns the new ones are initialized to maintain the spatial speed and density profile.

When there are subdivisions of varying sizes present, it becomes advantageous to integrate each one at its maximum allowed time step. This step is set by the stability limit (Equation 6). Such integration is accomplished through nonsequential calculations of the subdivisions. In this scheme the time argument of each state variable remains as near to the others as possible. The time arguments of all state variables are identical at user-set intervals so that valid outputs can be printed.

For example, consider a region of length 0.01 mile between regions of 0.1 and 0.2 mile. At the start each region would be integrated with its respective time step. Then the 0.01-mile region would be stepped forward in time by nine of its steps. At this point both the 0.01- and the 0.1-mile regions would be calculated. Then the 0.01-mile region would be integrated nine more times. Finally, all three regions would be calculated.

These asynchronous calculations are valid only if the subdivisions are properly discrete. In this case the only subdivisions that change quickly are the short ones. The stability limit ensures that these regions are integrated at a rate that maintains causality. The validity of this scheme can be shown by comparing results of nonadapted simulations with those of simulations where the adaptation is used.

Return to the lane drop simulation of Figure 3. In the acceptable simulation of Figure 8 and Table 6 the freeway was divided into 100 subdivisions each with a length of 0.01 mile. The stability limit restricts the time steps for these divisions to 0.2 sec. Therefore, the 10-min simulation requires 100 subdivisions to be calculated 3,000 times each. These 300,000 calculations of the state equations took 4.3 min of CPU time on a DEC VAX11/750.

Figure 13 and Table 10 give the simulation results for the same situation using the adaptive scheme. The spatial and temporal steps were adapted at each minute during the simulation. The total number of calculations of the state equations was 3,700. The simulation result remained virtually unchanged from the nonadaptive one, and the running time was reduced to 50 sec.

In general, the use of this spatial and temporal step size adaptation scheme results in large savings of computer time and does not jeopardize the model's accuracy. The savings is even greater in simulations of real freeways than in the lane drop example. This is because there are often large regions where there is no congestion; longer subdivisions can be used in these areas. For example, the 3-hr simulation of the

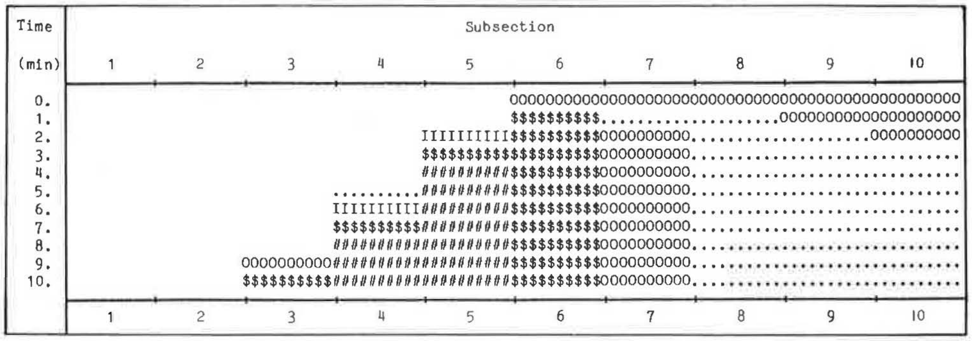


Legend For Contour Map

| Lower Limit | Upper Limit | Symbol |
|---|---|---|
| 0. | 40. | |
| 40. | 50. | . |
| 50. | 60. | O |
| 60. | 80. | I |
| 80. | 120. | $ |
| 120. | 1000. | # |

**FIGURE 13 Subsection averaged density (vehicles/mile-lane)--continuous equilibrium relation with $\Delta x$ = adaptive.**

Santa Monica Freeway (February 17, 1981) now would require 1 hr 50 min of CPU time on a DEC VAX11/750. This is a reduction by a factor of 21 from the non-adaptive simulation. Of this CPU time, only 3 percent is used in setting the adaptive spatial and temporal steps. The run time is not a fixed value because the number of subdivisions needed with the adaptive module depends on the congestion level.

There are some interesting benefits to using the adaptive scheme included in FRECON. First, it is possible to place special subdivisions at detector locations. They give true local information as would a real roadway detector. The ability to include realistic detectors in a macroscopic model greatly influences the results of tests with on-ramp controllers that use detector information. Second, because each subdivision acts as a miniature subsection within the model, a selected subdivision can be used to duplicate capacity loss during an incident. In this way the incident is localized instead of spread over an entire subsection. These alterations are handled within the adaptive module and require only conventional user inputs.

This adaptive scheme has been successful, but the adaptation relies on presumed consequences of given geometries and flows. Therefore, it must by nature be conservative. If there is any doubt, shorter subdivisions are applied. This ensures that the next flows examined by the adaptive module are, in fact, valid. The following adaptive scheme avoids this overcautiousness and results in a more elegant and natural discretization.

## A MORE NATURAL ADAPTATION

To avoid the conservative subdividing present in the heuristic adaptation scheme and to provide a clearer and more natural adaptation, the model has been reformulated into a Lagrangian reference frame (9). Here all changes are measured relative to a particle in motion with the local flow. This differs from the stationary (Eulerian) reference frame used in many fluid flow problems. In the Lagrangian frame the discretization can become a natural part of the state equations, causing many of the adaptive problems to disappear.

Start by transforming the model of Equations 1 and 2 into the Lagrangian frame:

**TABLE 10 Volume Leaving Subsections (Vehicles/Hour)--Continuous Equilibrium Relation with $\Delta x$ = Adaptive**

| Time | Subsection Number | | | | | | | | | |
|---|---|---|---|---|---|---|---|---|---|---|
| (min) | 1 | 2 | 3 | 4 | 5 | 6 | 7 | 8 | 9 | 10 |
| 0 | 4455 | 4455 | 4455 | 4455 | 4455 | 4000 | 4000 | 4000 | 4000 | 4000 |
| 1 | 4468 | 4465 | 4463 | 4461 | 4368 | 3963 | 3975 | 4003 | 4001 | 4000 |
| 2 | 4487 | 4486 | 4484 | 4483 | 3938 | 3980 | 3941 | 3972 | 4011 | 4003 |
| 3 | 4495 | 4494 | 4494 | 4493 | 3969 | 3971 | 3965 | 3957 | 3985 | 4020 |
| 4 | 4498 | 4498 | 4498 | 4489 | 3968 | 3970 | 3969 | 3966 | 3970 | 4004 |
| 5 | 4499 | 4499 | 4499 | 4202 | 3969 | 3970 | 3970 | 3969 | 3970 | 3980 |
| 6 | 4500 | 4500 | 4500 | 3957 | 3969 | 3970 | 3970 | 3970 | 3970 | 3972 |
| 7 | 4500 | 4500 | 4499 | 3970 | 3969 | 3970 | 3970 | 3970 | 3970 | 3970 |
| 8 | 4500 | 4500 | 4435 | 3970 | 3969 | 3970 | 3970 | 3970 | 3970 | 3970 |
| 9 | 4500 | 4500 | 4048 | 3969 | 3969 | 3970 | 3970 | 3970 | 3970 | 3970 |
| 10 | 4500 | 4500 | 3970 | 3969 | 3969 | 3969 | 3970 | 3970 | 3970 | 3970 |

$$(\partial\rho/\partial t) + [\rho(\partial u/\partial x)] = S(x,t) \tag{8}$$

$$(\partial u/\partial t) = [(1/c)u_e(\rho) - u] - [b(1/\rho)(\partial\rho/\partial x)] \tag{9}$$

In this form the convective terms are no longer present because the observer moves with the flow.

Before the discretization of the model, consider a local region of constant mass (vehicles) but changeable length and density:

$$V = \rho \cdot \delta x \tag{10}$$

where

V: number of vehicles in region $\delta x$ and
$\delta x$: length of region.

If the problems of on- and off-ramps are ignored for the moment (which would alter the fixed number of vehicles in the region), it is possible to transform the conservation relation (Equation 8) into a form based on the length of the constant vehicle region:

$$[\partial(\delta x)/\partial t] = (\delta x) \cdot (\partial u/\partial x) \tag{11}$$

Further, the length of the region can become the model's discrete spatial step. These discrete regions will be referred to as a "box" to emphasize their constant vehicle number (when not near a ramp). In this case the discrete model is

$$\delta x(x,t+\Delta t) = \delta x(x,t) + \Delta t\,[u(x+\Delta x,t) - u(x,t)] \tag{12}$$

$$u(x,t+\Delta t) = u(x,t) + \Delta t\,\Big((1/c)\,[u_e(\rho) - u(x,t)] - b \cdot [1/\rho(x,t)]\,\{[\rho(x+\Delta x,t) - \rho(x,t)]/\Delta x\}\Big) \tag{13}$$

where

$\rho(x,t) = V/\delta x(x,t)$

Note that the discrete regions (boxes) are no longer fixed on the freeway; they now travel with the flow and lengthen or shorten as the local density changes. It is this natural altering of the box lengths that provides the spatial adaptation.

In this particular model, special care must be taken when each box passes a ramp (the number of vehicles in the box changes) and when it passes a lane drop or add (the box's density changes). In addition to solving Equations 12 and 13, each box's position must be updated at each time step. The critical length of the boxes is still 0.01 mile (at their highest density) and the stability limit remains the same as in the heuristic scheme.

The use of temporal adaptation with this form of the model also requires care. Previously, all subdivisions maintained their size for a set period of time. In this scheme, the boxes vary their lengths at each time step. Still it is possible to find time periods (5 to 10 sec) over which the boxes do not change their sizes significantly. A temporal adaptive scheme like the one used in the heuristic method can be used if it is updated at intervals of 5 to 10 sec.

In implementing this adaptive scheme, a few points must be considered. The upstream boundary condition is now provided by the creation of boxes waiting to approach the freeway section. The downstream boundary condition is met by allowing boxes to completely exit the freeway before they are no longer considered part of the simulation. The number of vehicles in the boxes is set by the queueing density, the number of lanes, and the maximum allowed spatial step during congestion (0.01 mile for this model). As the boxes pass ramps the number of vehicles they contain changes. These changes must be monitored at regular intervals so the discretization limit will not be violated. When a limit violation occurs, the boxes on the freeway are reformed and initialized so that the simulation progresses smoothly and the model's accuracy is maintained.

Natural adaptation of the spatial steps permits the use of realistic detectors and localized incidents as in the heuristic scheme. The inherent nature of the spatial adaptation and the accuracy that results reduce the computing times for this scheme. However, the temporal steps must be set more often because the spatial steps vary continually. The net effect is that simulation tests have shown this method to give accurate results with savings of 10 to 20 percent over the heuristic adaptive scheme. In cases where the demands have a high frequency component, this natural adaptation is better suited and gives savings as high as 50 percent in the run times.

## CALIBRATION AND VALIDATION OF FRECON

The preceding discussion of how to properly discretize a freeway model is of interest only if the resulting model can duplicate the behavior of a real-world freeway. The Santa Monica Freeway (I-10) in Los Angeles was selected as the test site for the calibration and validation of the FRECON model. This selection was greatly influenced by the desire to use a site that would also be compatible with later comparative studies of control strategies (1).

The study site is a 7.7-mile, eastbound section from the San Diego Freeway (I-405) heading toward downtown (Figure 14). The hours of operation examined were the "counterpeak" from 3 p.m. to 6 p.m. This section is part of the Los Angeles 42-mile-loop surveillance system so main-line and ramp-detector information was available. Data sets were provided for 5 weekdays during the winter of 1981 that were believed to be normal and incident free. Each contained main-line input and on- and off-ramp flows at 5-min intervals. Also, a set of 35 mph contours from the main-line detectors was provided for each day. The first day of data was to be used to calibrate the model's capacities and the remaining 4 were for validating the model's performance. The roadway geometry and detector locations used in the modeling were obtained from detailed maps and field visits.

Using the first day of data (February 17, 1981), the model's capacities were tuned. The calibration was performed by comparing the field detector's 35-mph contour with that of the model's detectors. Figure 15 shows the result of this comparison for the calibrated capacities. The 35-mph contour is generally a reliable indicator of the extent of main-line queueing. In general, the model and field contours show a similar extent of main-line queueing.

The unusual field contour at detectors 9 and 10 (subsection 11) is due to an unusual field geometry. Subsection 11 is bypassed by a collector-distributor road that also carries a high percentage of through traffic. This causes subsection 11 to be a bottleneck. The field configuration is modeled with the collector-distributor through traffic being carried on the model's main line. The unusual congestion contour is caused by merging patterns. This results in a model capacity for subsection 11 that is 16 percent lower than that of neighboring subsections. This modeling approximation cannot duplicate all of the field behavior around detectors 9 and 10.

When the model capacities were once calibrated on the first day's data, they remained fixed for the validation study. Figure 16 shows a comparison of the model and field 35-mph contours for one of the validation days (February 23, 1981). As with the calibration day, the two contours show similar patterns for the upstream bottleneck (detectors 1-4). Also, there is difficulty matching the field pattern around detectors 9 and 10 because of the modeling of the field geometry. The other three validation days also showed field-model contour compatibility as shown in Figure 16.

The five simulations of the Santa Monica Freeway resulted in a range of total travel times from 3,321 to 4,528 vehicle-hours and total services from 163,000 to 176,000 vehicle-miles. For all five simulations the model was able to duplicate the overall field congestion pattern. This was possible over this range of traffic demands because of two properties of the model. First, it is properly discrete. Hence, it can follow the density-space profile that is present during congestion. Second, the model uses localized point detectors. It is possible to duplicate the sudden changes in detector state as the main-line queue passes over only if the detector has a restricted, local range.

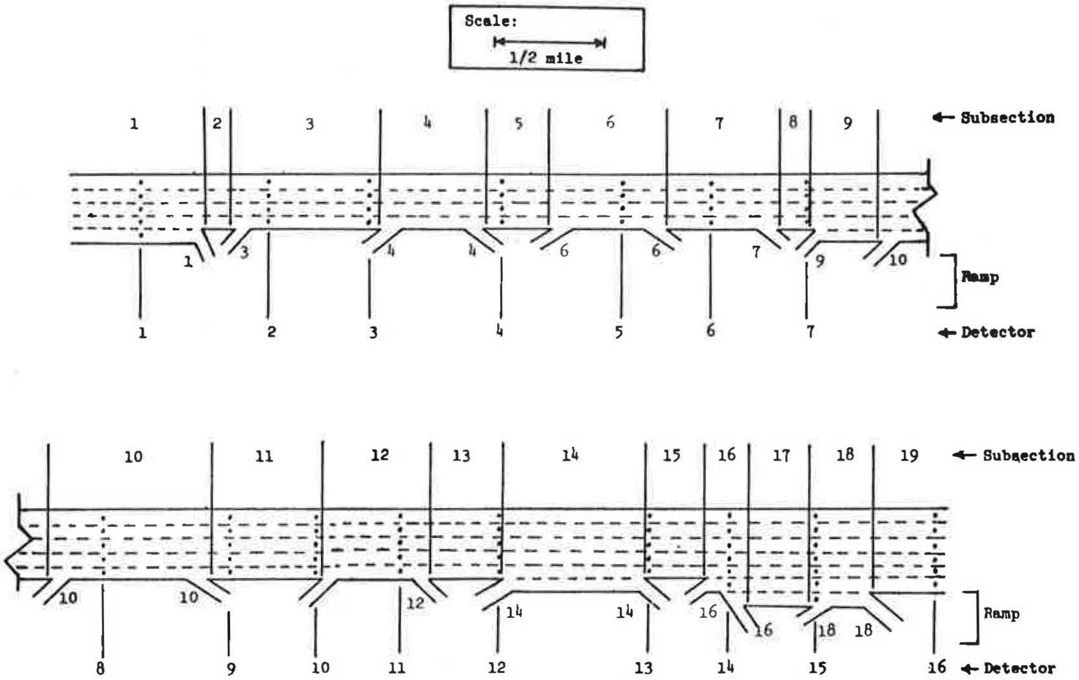


FIGURE 14 Santa Monica Freeway geometry.

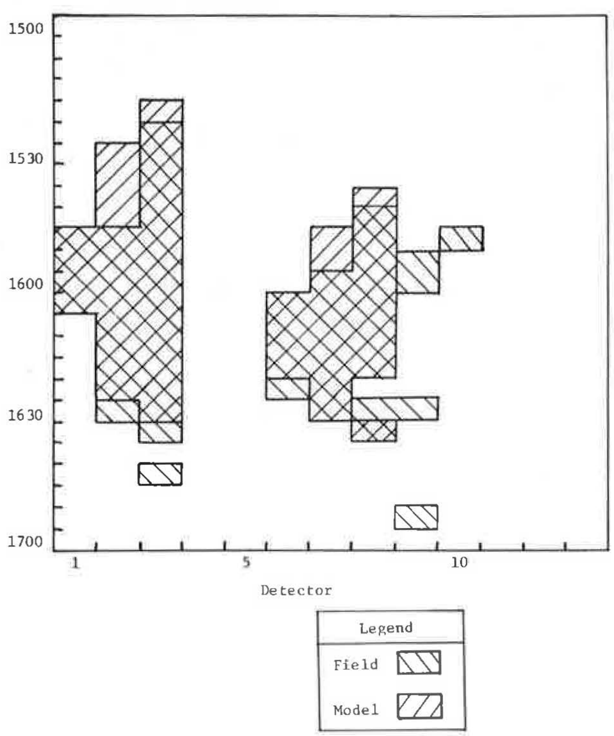


FIGURE 15 Santa Monica Freeway detectors < 35 mph—February 17, 1981.

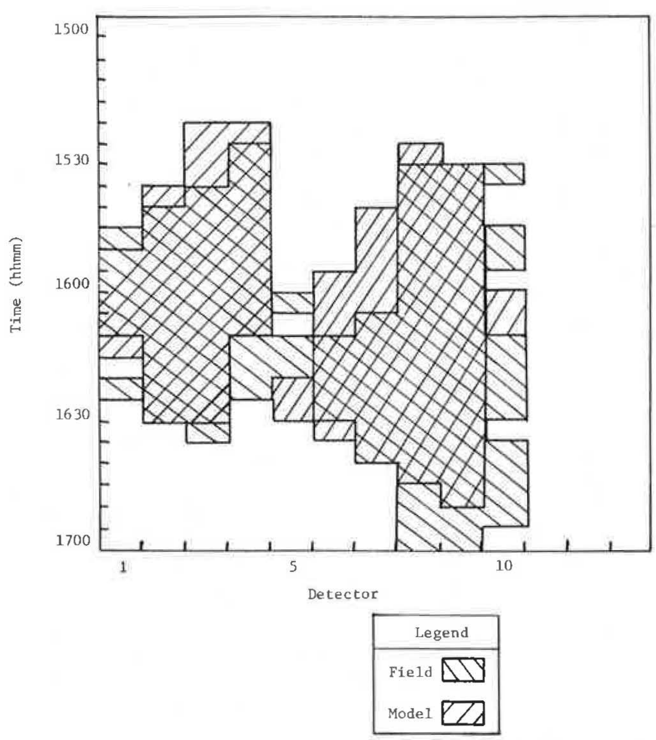


FIGURE 16 Santa Monica Freeway detectors < 35 mph—February 23, 1981.

## SUMMARY

All discrete models have limits on the maximum allowable step sizes. This limit must be adhered to if the model is to be a faithful representation of the original continuous model or the real world. If the intervals are larger than the permitted maximum, the simulation results are irrelevant and merely an artifact of improper discretization. Proper discretization creates a model the results of which are an accurate approximation of the continuous solution. The model must be made properly discrete before its parameters can be tuned and the resulting model calibrated.

When freeway models have terms like those in FREFLO, the proper discretization is not the traditional subsection. Although the concept of a subsection (the region between geometric features on the roadway) is useful for model input and output, it is usually an invalid mathematical discretization. In particular, the anticipation term of the model limits the size of the spatial steps permitted so that changes in the density-space gradient can be followed. To ensure that shock fronts at the boundary of main-line queueing are modeled properly, spatial step sizes must be less than or equal to 0.01 mile. This subdividing is made necessary by mathematical limitations. It can be performed internally in the model so that the user can continue to interact with the model using traditional geometric subsections.

The direct application of this proper spatial discretization and the proper temporal step sizes needed to maintain the model's stability result in excessive computer run times. Because the discretization is limited by changes in the density-space slope, it is possible to find circumstances where the spatial step sizes may be lengthened without an adverse effect on the simulation results. These occur when the density is low and the density-space gradient is constant. When this situation is identified, it is possible to adjust the spatial and temporal steps the model uses, thereby increasing its efficiency.

These ideas motivated the development of the adaptive modules used in the FRECON model. The first is a heuristic scheme where flow levels and geometry are examined and compared with a library of required subdivision patterns. In this way the spatial steps are adjusted at regular intervals so that the maximum allowed steps are always used. When these spatial steps have been established, the corresponding maximum temporal steps that ensure stability are known. Therefore, by using these asynchronous time steps, it is possible to reduce the number of times each subdivision state needs to be integrated.

The second adaptive scheme is more natural because it is built into the mathematics. By transforming the model from a stationary reference frame to a moving one, it is possible to define regions that move with the flow of traffic. Each region is discretized into a "box" that contains a constant number of vehicles and a length that is inversely proportional to its density. This natural variation of length with density provides the spatial adaptation. A scheme similar to the heuristic adaptation is used to reduce the frequency of the integration steps required.

Both of these adaptation schemes have proven useful in reducing the computing time required for a simulation. The first scheme, used in the FRECON model, reduced the CPU time for a typical simulation by a factor of 21. Further, the presence of an adaptive scheme permits the use of realistic local detectors and localized incidents in the model.

The FRECON model was calibrated on the Santa Monica Freeway for a 3-hr peak period. The calibration of model capacities was performed by comparing field and model detector 35-mph contours. These capacities, and the model's performance, were then validated using four more peak periods of data from the same freeway. With the exception of a complex collector-distributor geometry, which could not be accurately modeled, the simulation results generally agreed with the field data.

The performance of the FRECON model on the 4 days of validation indicated that the model can duplicate freeway behavior over a wide range of demand levels and can realistically model the response of localized detectors. These properties have proved helpful in studying the use and design of freeway control strategies.

## ACKNOWLEDGMENT

This research was supported in part by the California Department of Transportation and the FHWA under grant F80-T003.

## REFERENCES

1. P.S. Babcock, A.D. May, D.M. Auslander, and M. Tomizuka. Freeway Simulation and Control. Research Report UCB-ITS-RR-82-13. Institute of Transportation Studies, University of California, Berkeley, 1982.
2. H.J. Payne. Models of Freeway Traffic and Control. Mathematics of Public Systems, Vol. 1, No. 1, 1971, pp. 51-61.
3. H.J. Payne. FREFLO: A Macroscopic Simulation Model of Freeway Traffic--A User's Guide. ESSCOR, San Diego, Calif., 1978.
4. H.J. Payne. FREFLO: A Macroscopic Simulation Model of Freeway Traffic. In Transportation Research Record 722, TRB, National Research Council, Washington, D.C., 1979, pp. 68-77.
5. W.F. Phillips. A Kinetic Model for Traffic Flow with Continuum Implications. Transportation Planning and Technology, Vol. 5, 1979.
6. W.F. Phillips. A New Continuum Model for Traffic Flow. Final Report DOT-RC-82018. Utah State University, Logan, 1979.
7. H.J. Payne, W.A. Thompson, and L. Isaksen. Design of a Traffic Responsive Control System for an L.A. Freeway. Transactions on Systems, Man, and Cybernetics, Vol. SMC-3, No. 3, May 1973, pp. 213-224.
8. A. Ceder. A Deterministic Traffic Flow Model for the Two-Regime Approach. In Transportation Research Record 567, TRB, National Research Council, Washington, D.C., 1976, pp. 16-30.
9. K.R. Symon. Mechanics. Addison-Wesley, Reading, Mass., 1971.

Publication of this paper sponsored by Committee on Traffic Flow Theory and Characteristics.